



Supporting Information (SI)

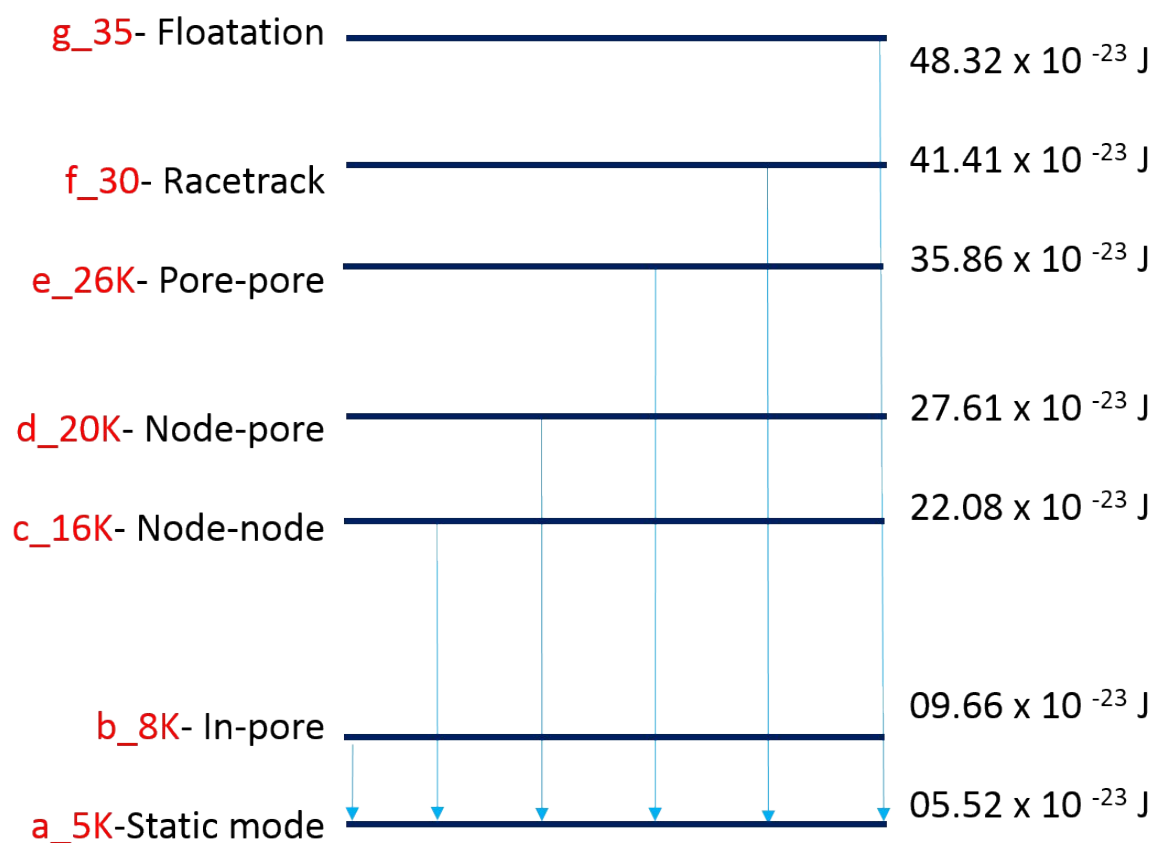
Watching nanostructure growth: Kinetically controlled diffusion and condensation of Xe in a surface metal organic network

Aisha Ahsan,^a S. Fatemeh Mousavi,^a Thomas Nijs,^a Sylwia Nowakowska,^a Olha Popova,^a Aneliia Wäckerlin,^a Jonas Björk,^{*b} Lutz H. Gade,^{*c} and Thomas A. Jung^{*a,d}

Contents

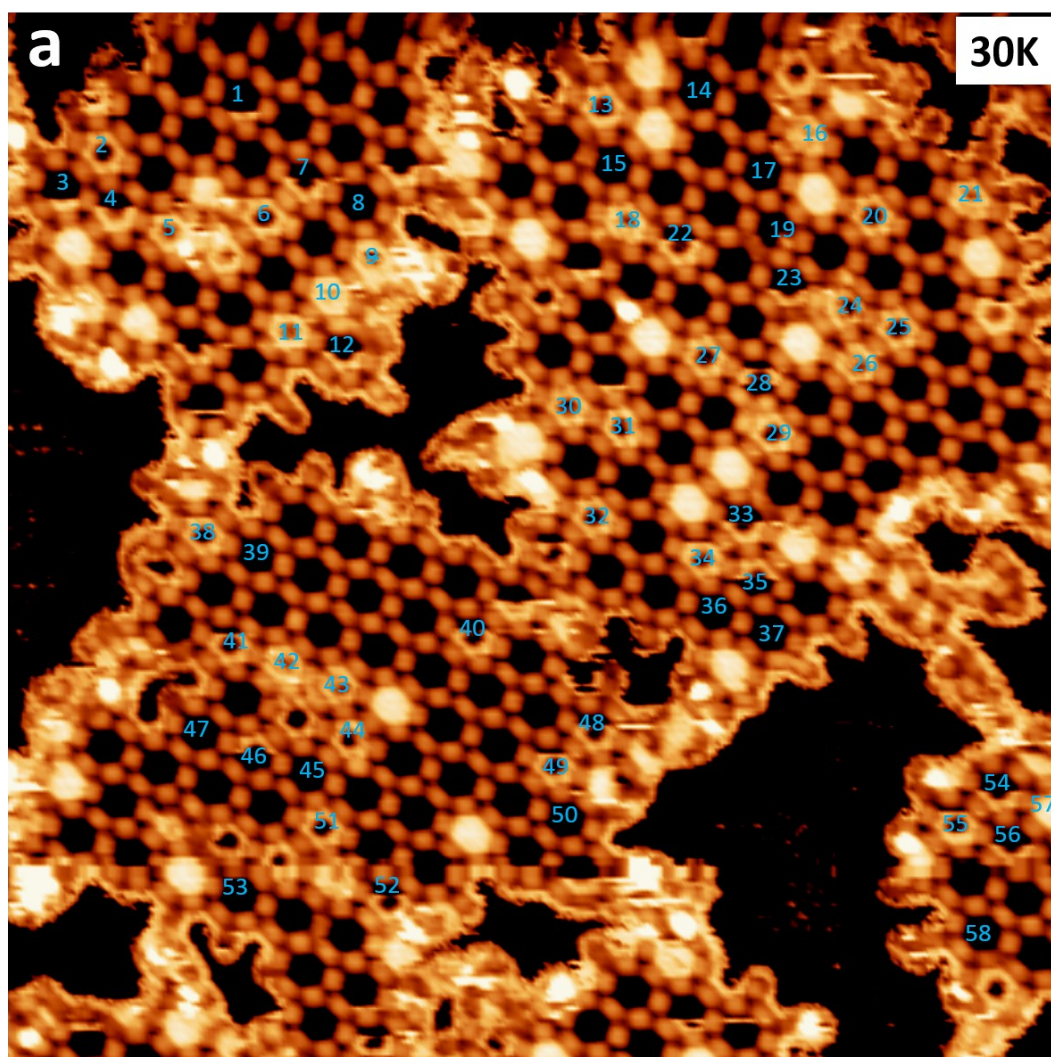
1. Energy landscape of diffusion pathways	SI-G1
2. Coarsening of Xe condensates in DPDI networks	SI-1
3. Evolution of Xe diffusion patterns	SI-2
4. Different diffusion modes	SI-3
5. Coarsening of Xe condensates	SI-4
6. Coverage dependent diffusion	SI-5
7. Graph, exposure dependent filling up pores	SI-G2
8. Calculated Xe pathways	SI-6
9. Arrhenius activation processes	SI-7
10. Calculations of pore occupancies	SI-8

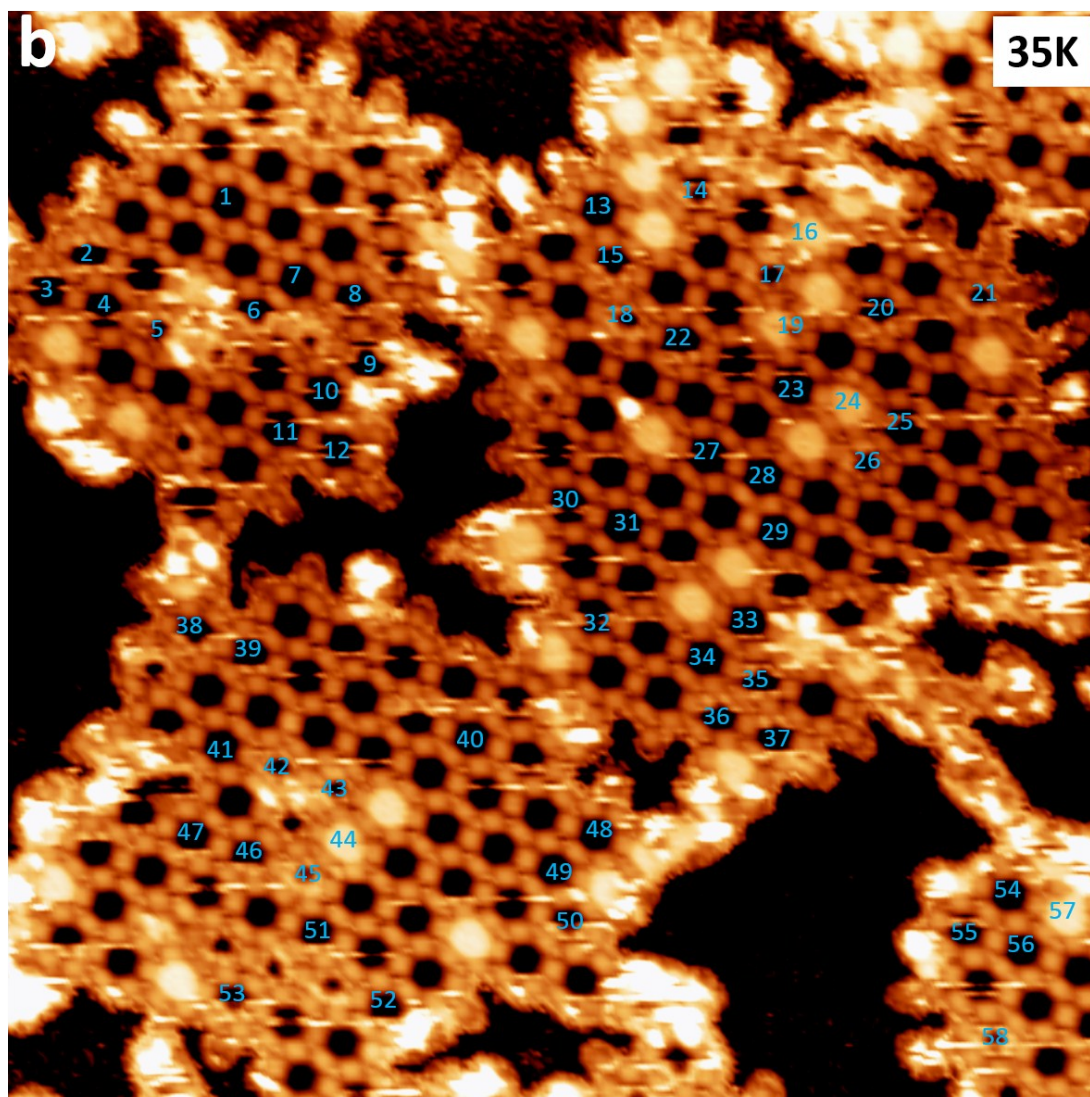
1. Energy level landscape for different pathways of diffusion and coarsening



SI-Graph1: Energy (kT) level landscape of coarsening pathways. This graph shows the trend of increasing energy with different levels of diffusion.

2. Coarsening of Xe condensates in networks DPDI

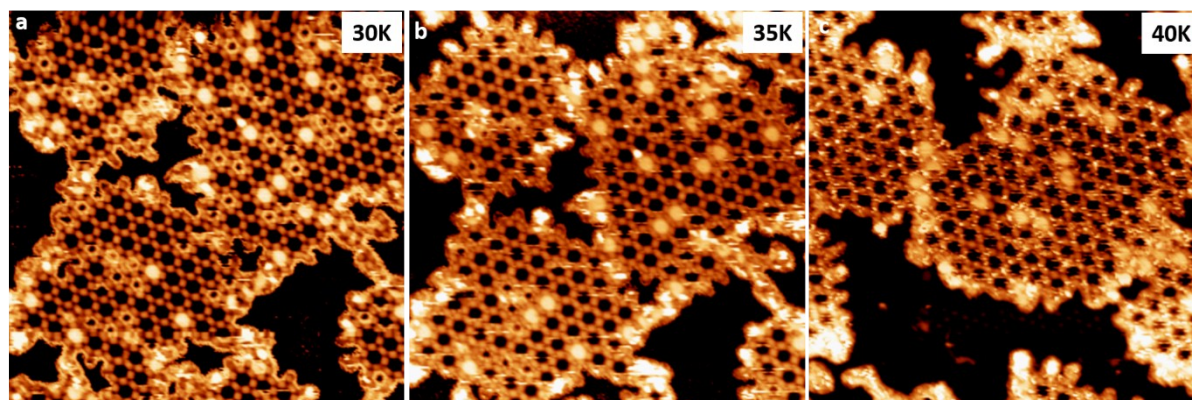




Temperature	n=12	n < 6	n > 6
30K	9%	5%	7%
35K	12%	2%	24%

SI-1: Coarsening of Xe condensates in DPDI networks. (a) STM image taken at 30 K revealing the mobility of Xe within-pores and along the rim around the networks. The two dimensional diffusion of Xe over networks at 30K is associated with transient mobility. Different pores are numbered in blue (a) at 30K with the exactly corresponding pores labelled in the same way in (b) at 35K. The evolution of the occupancy of these pores has been listed in a table of which the summary is shown at the bottom of the figure. Clearly there is the trend of partially filled pores, both at lower than 6 occupancy (will be emptied) and at higher than 6 occupancy (will be filled) to disappear while the number of completely filled pores is increasing. STM scanning parameters ($V=1$ V, $I=10$ pA, image size 35nm x 35nm)

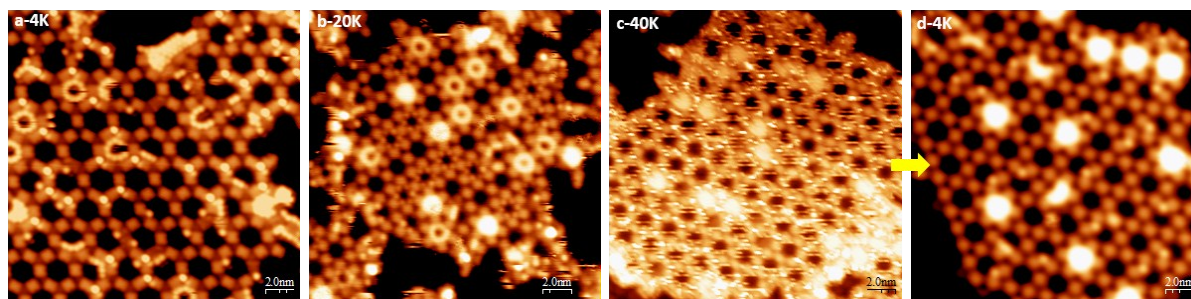
3. Evolution of Xe diffusion patterns



Temperature (K)	30K	35K	40K
Collision events ($n_{\text{coll}} / \text{line}$)	$2.9 \times 10^4 n_{\text{coll}} / \text{line}$	$5.1 \times 10^5 n_{\text{coll}} / \text{line}$	$5.0 \times 10^6 n_{\text{coll}} / \text{line}$

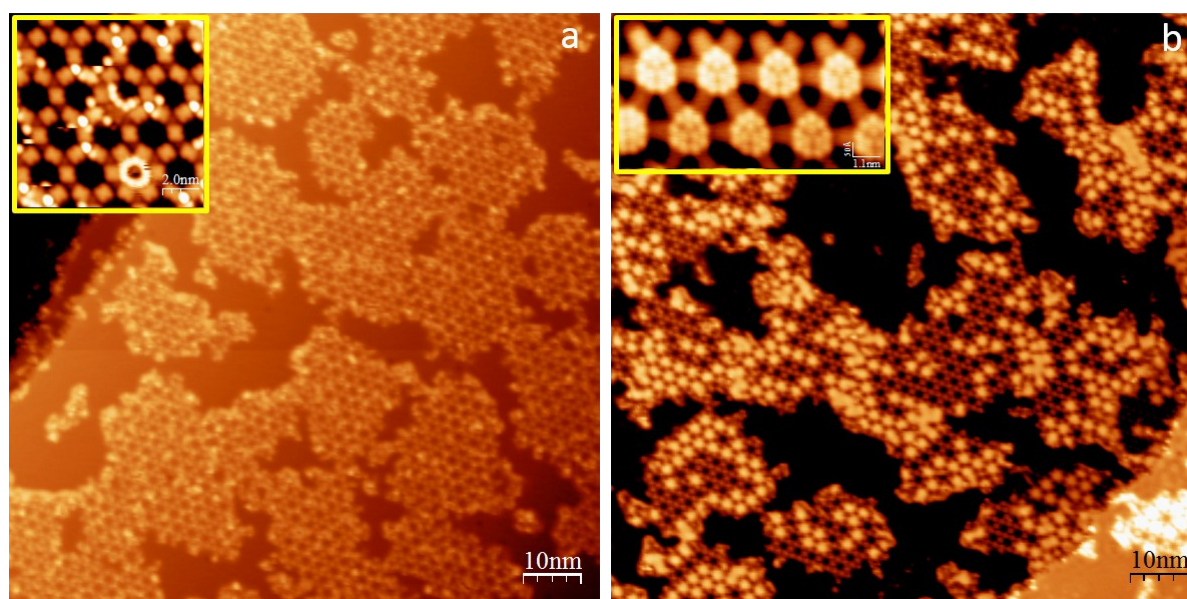
SI-2: Sequence of consecutive images showing the evolution of Xe diffusion patterns: **a)** at 30K, diffusion is predominantly occurring either inside the pores or along the network border. Pores with occupancies below 6 are recognized by ring like features with the STM virtual height dependent on the population of the number of diffusing Xe atoms. Pores with occupancy higher than 6 display disk shape patterns due to the presence of Xe which is closer to the center of the pore and the progressive shift of the quantum well state facilitating 2D diffusion inside the pore. A very low number of tip excursion ‘streaks’ is visible as the STM tip is scanning across the network backbone. **b)** at 35K, the diffusion along the outer rim is far less apparent, the coarsening of the filling patterns leads to less ‘ring shape’ and more ‘disk shape’ features. Indicating the coarsening pathway are the ‘streaks’ visible on the backbone of the DPDI network. We assign these ‘streaks’ to the presence of Xe diffusing along the network backbone, -and therefore forming a dynamic equilibrium between the pores of the different population which then results in the coarsening. From the scanning speed (36 nm) and the average length of the streak features in this data (~ 1.3 nm) we estimate a residence time of Xe to be in the order of some msec at the observation temperature. Note that this is only a rough estimate in presence of the electric field induced by the scanning tip among other potentially present interactions. **c)** at 40 K the mobile chains along the outer periphery of the network islands are completely gone and the number of ‘streak’ incidents increased even more significantly. The occurrence has been analysed by number of streaks (counted twice because of right and left STM tip scan) multiplied by area of scan, and the increased number of streaking frequency $10^4 n_{\text{coll}} \rightarrow 10^5 n_{\text{coll}} \rightarrow 10^6 n_{\text{coll}}$ as it evolves from 30K \rightarrow 35K \rightarrow 40K, respectively. This has been listed in the table below the figure. Note that there are no visible incidents of Xe adsorbing or diffusing across the Cu substrate at all these observation temperatures. STM scanning parameters ($V=1$ V, $I=10$ pA, Time per line = 972.8 msec, scan speed 35 nm/sec, image size 35nm x 35nm, pixels = 256 x 256)

4. Different diffusion modes



SI-3: Diffusion from nodes, in-pore mobility, start-up of coarsening ended up with maximization of pore filling with Xe atoms. (a) Xe atoms are static over nodes, in pores and around the networks at 4K with 0% dynamicity also 27% nodes occupancy with 48% pores occupancy. At 20K mostly atoms are mobile inside pores but not outside the networks with 0% dynamic channels. After annealing to 40K (c) and scanned back to 4K reveals most of pores are occupied with maximum 12 Xe atoms. STM scanning parameters ($V=1$ V, $I=10$ pA, image size 35nm x 35nm)

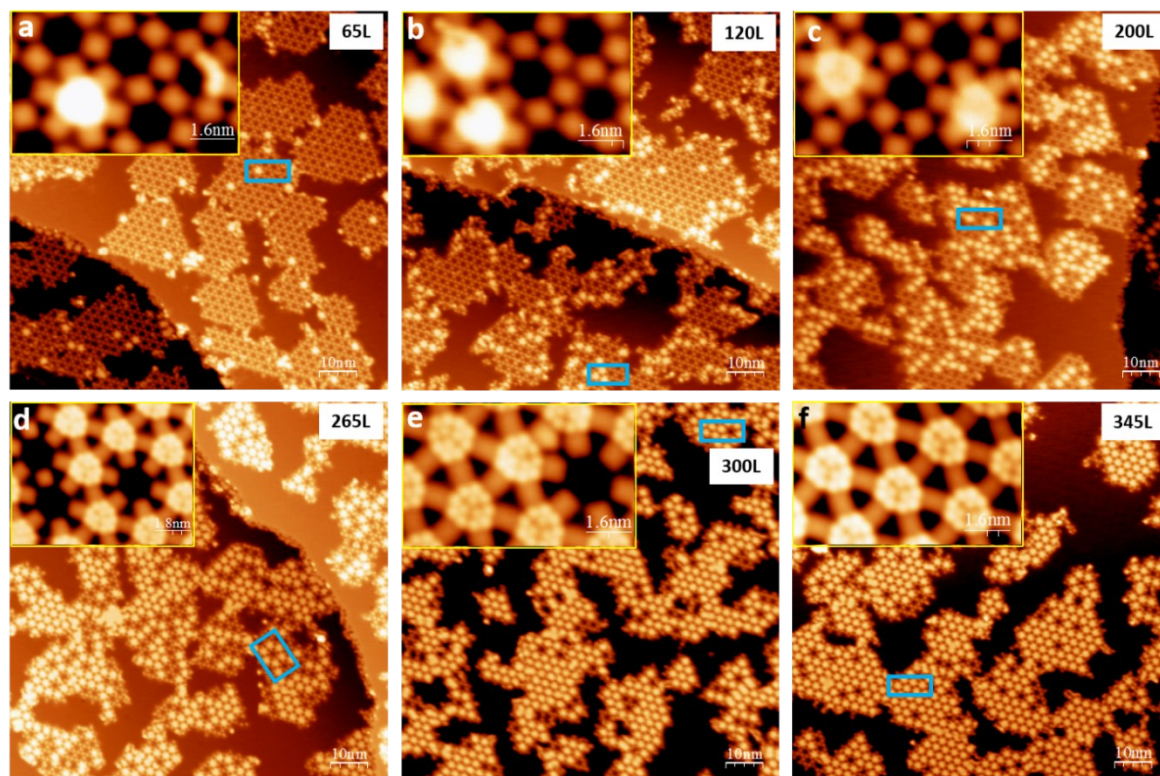
1. Coarsening of Xe condensates



SI-4: Coarsening of Xe condensates in network cavities. (a) STM image of network islands on Cu(111) after exposure with 240L-Xe. An irregular pattern of different adsorption sites is hosting the Xe: at the nodes on the network, in the pores with different occupancy, and also on the bare Cu(111) surface, but the latter only in small areas around the network boundaries. (b) after annealing to 40K for 30 minutes and STM inspection at 4K most of the Xe is found in fully (12-fold) occupied pores. Only some small or

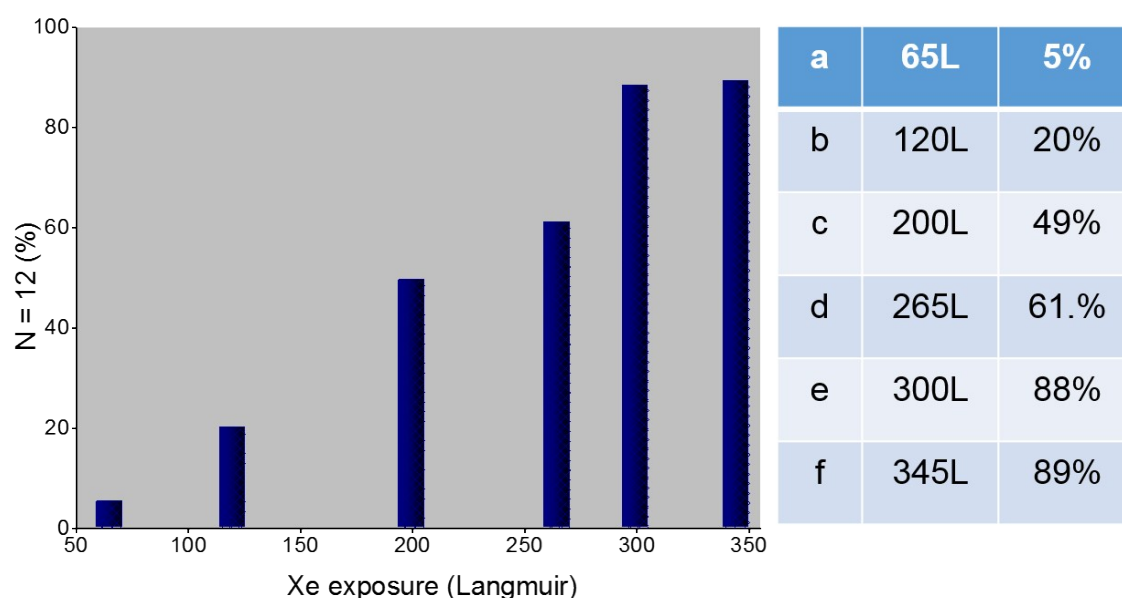
narrow pockets between neighbouring network islands are covered by larger Xe islands which are imaged by featureless bright areas. STM scanning parameters ($V=1$ V, $I=10$ pA, image size 100 nm X 100 nm).

5. Coverage dependent diffusion



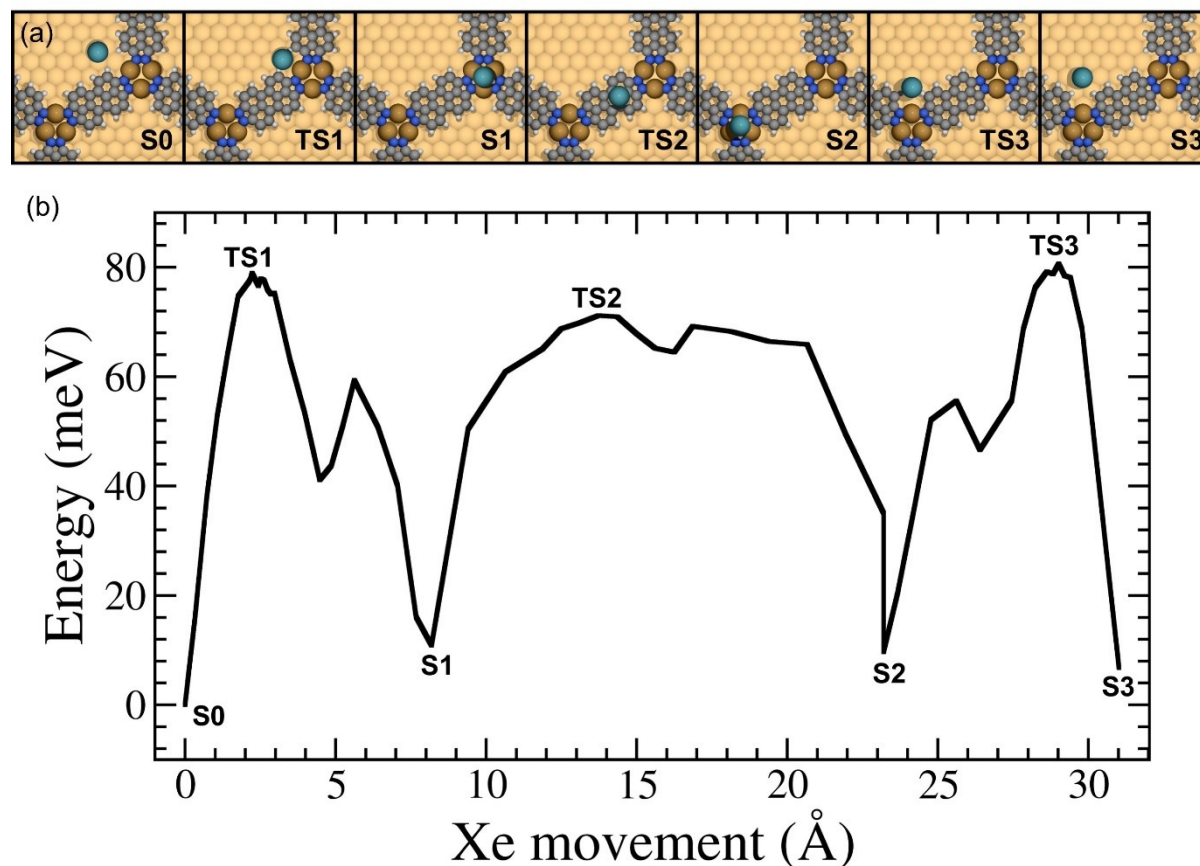
SI-5: Coverage dependent diffusion studies in DPDI networks. (a) with 65L exposure of Xe, some pores are fully saturated by Xe atoms and few with different occupancies while most of them are empty that is clearer in inset. (b) 120L exposure of Xe the ratio of fully filled pores is increased but still have with high ratio of partially filled pores indicated in inset. This trend of filling up pores to their maximum capacity gradually increase from 50%, 61%, 88% to 89% with increasing exposure with 200L (c), 265L (d), 300L (e) and 345L (f) respectively while this trend is also clear from the graph below the figure. All samples are exposed to Xe at 9K with follow up annealing to 40K for 30 minutes and scanned back at 4K. STM scanning parameters ($V=1$ V, $I=10$ pA, image size 100 nm X 100 nm, inset images 8nm x 5nm)

7. Graph, exposure dependent filling up pores



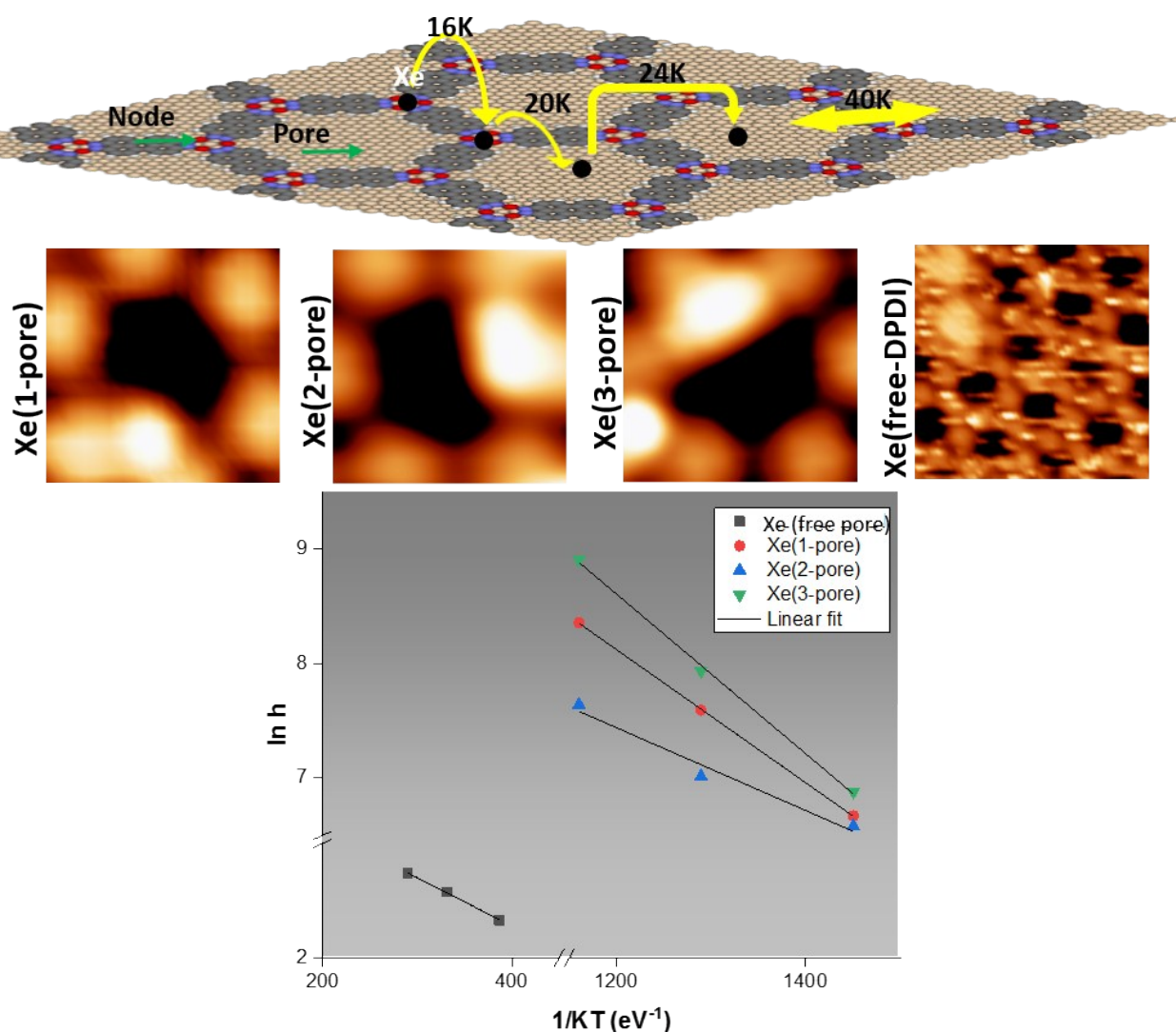
SI-Graph2: Exposure dependent filling up of pores with Xe atoms by diffusion in DPDI networks. This trend of filling the pores based on diffusion/coarsening procedure shows from the graph, increases with increasing the exposure of Xe atoms over the sample. Letters a, b, c, d, e and f correspond to images a, b, c, d, e, f in figure S5.

8. Calculated Xe pathways over DPDI networks



SI-6: Raw data from the calculated pathway of the Xe moving across the surface network. (a) Top and side views of local minima (**S0-S3**) and transition states (**TS1-TS3**) following the nomenclature in Figure 5 of the manuscript, together with the full energy profile between the states, with the position of the relevant states indicated. Notably, the two steps associated with pore-to-node motion (**S0-S1** and **S2-S3**) are associated with two barriers and for simplicity only the effective barriers are reported in Figure 5.

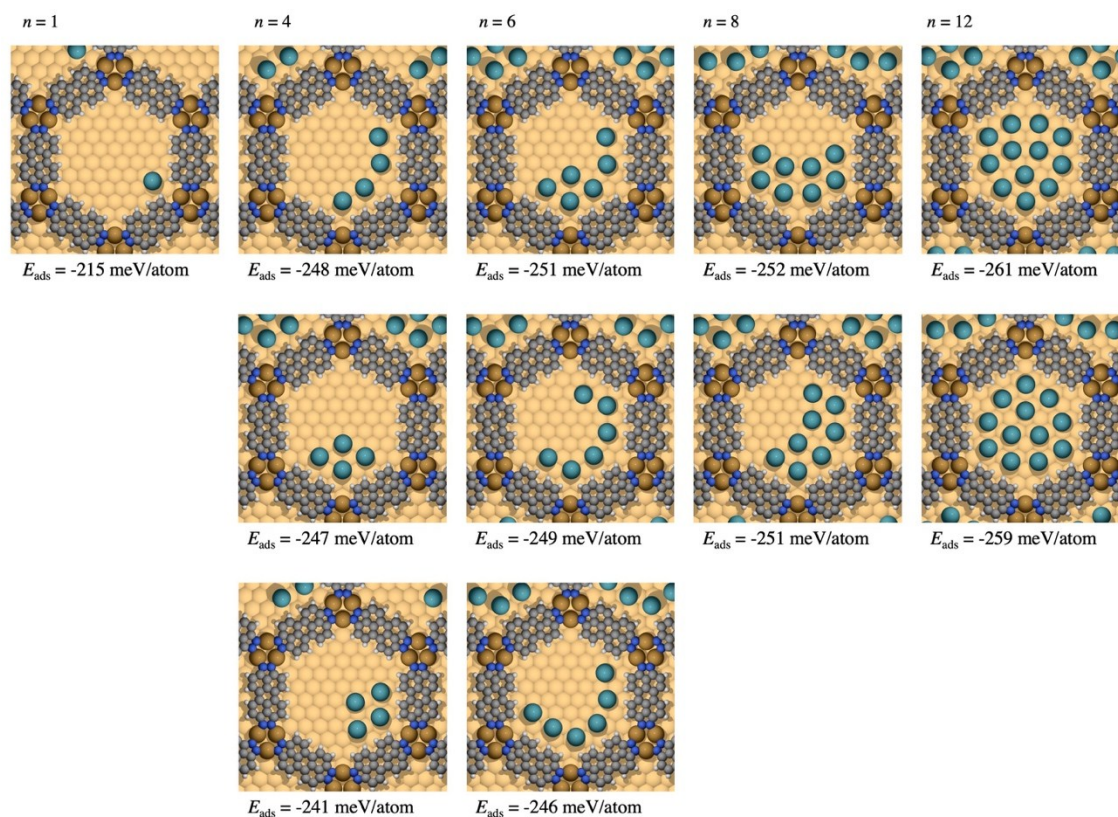
9. Arrhenius activation of hopping processes



SI-7: Hopping processes observed for 1 and 3 Xe atoms in the confinement ($\text{Xe}_{(1, \text{PORE})}$ and $\text{Xe}_{(3, \text{PORE})}$) respectively, and for Xe running along the DPDI backbone at elevated temperatures ($\text{Xe}_{(\text{free}, \text{DPDI})}$). Three

fundamentally different processes can be identified by their activation energies and prefactors/attempt frequencies as they are summarized in **Table SI-7** below. The in-pore diffusion of **Xe_(1, PORE)** and **Xe_(3, PORE)** can be discriminated by i) a higher E_{ACTIV} of the Xe(3) condensate which initially diffuses as a trimer and by ii) a slightly lower rate constant of the same Xe(3) constant. Notably, the activation energy for the rather weakly bound, individually diffusing Xe atoms on top of the DPDI is determined to be the lowest. These results are plausibly consistent with the facts that **Xe_(1, PORE)** and **Xe_(3, PORE)** are bound to a considerable potential by the metal substrate, the confining DPDI and the electronic state in the pore (S. Nowakowska et al. Nature Communications). This affects both the pre-factor / attempt frequency as well as the activation energy. The former scales with the 'effective size' of the diffusing object and the latter scales with the increased observation of hopping processes with increased availability of thermal energy. It is important to note here, that once Xe reaches the position on the DPDI backbone it is very weakly bound i.e. 'effectively free' compared to the Xe hopping around inside the complex potential imposed by the porous confinement. Also note that these analyses are more exemplary due to the limited bandwidth of the STM method. The hopping processes can only be sampled for a few decades i.e. between msec and seconds. This does not allow for a precise quantification.

10. Calculations of pore occupancies



SI-8. Calculated adsorption energies per Xe atoms inside pore for different occupancies and configurations.

Sequence of DFT optimized pores occupied by 1, 4, 6, 8, and 12 Xe atoms, with corresponding adsorption energies, showing all considered adsorption configurations. Notably, there is a very small energy difference between having the atoms along the rim compared to having them clustered for $n=4$ and 6.